

other sphenoidal planes with the surface. Most of this detail is invisible in Fig. 6, although the hexagonal outline of the surface structures is sometimes quite distinct.

The clarity with which the step-by-step growth features can be observed (see cover, upper right) is further exemplified at a magnification which, in the normal mode (cover, upper left), is clearly unusable. Taken at lower power (cover, lower left and lower right), the Y-shift effect can be seen to introduce considerable difficulties in interpretation if complex morphology or topographical relief is present. Using a lower amount of modulation will reduce this effect (as shown previously, Figs. 2 and 3), but, taken in conjunction with the normal mode photograph, the Y-modulation mode photograph permits detailed examination of fine structure of selected areas.

We thus deduce that this method becomes increasingly important as higher and higher magnifications are employed, especially with magnetic materials or on surfaces with low or moderate relief, and that at lower magnification the Y-modulation photographs provide valuable information supplementing normal mode photographs.

There are many possible applications

of the use of this device—for example, examining and photographing the morphology and surface structure of very small crystals, such as those encountered in clay mineralogy. Stereo pairs made by this means will also be exceptionally useful.

Further, the Stereoscan may now be fitted with a spectrometer, and therefore be capable of electron-probe microanalysis. Under these conditions the output of the x-ray detector may be applied to the line scan in lieu of the photomultiplier output; this will produce a Y-modulation image which represents the distribution of the elements in the specimen analyzed in a three-dimensional form.

Finally, the scanning electron microscope will soon be fitted with a self-heating stage. This will enable us to examine magnetic minerals while heating them through their Curie points and to observe any changes taking place at that temperature.

T. K. KELLY
W. F. LINDQVIST

*Department of Mining Geology,
Royal School of Mines, Imperial
College, London, S.W.7, England*

M. D. MUIR

Department of Geology

6 February 1969

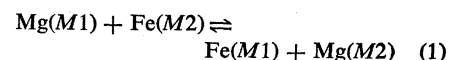
Cooling History of Orthopyroxenes

Abstract. *Order-disorder transitions between ferrous iron and magnesium in orthopyroxenes [minerals close to the composition (Fe,Mg)SiO₃] occur rapidly between approximately 480° and 1000°C. Disordering and ordering have been studied experimentally. The determination of the metastable ferrous iron site occupancy in orthopyroxenes from rapidly cooled volcanic rocks provides information on the cooling rates, especially from 600° to 480°C.*

Atomic order-disorder transitions in silicate crystals are often very sluggish. If the temperature changes rapidly, the atomic distribution over the nonequivalent sites may not be in accord with the equilibrium state at any instant. Below a critical temperature, the time needed to reach equilibrium will be very long and geological times may be needed to accomplish an equilibrated distribution. This is of special interest for the earth scientist since nonequibrated site occupancies may be found in nature which permit conclusions on the cooling history of the mineral. We have found that Fe²⁺,Mg order-disorder in orthopyroxenes is an unusually simple example which can be approached from the point of view of simple thermodynamical considerations.

Some features, however, are quite different from the order-disorder phenomena in silicates.

Orthopyroxenes are orthorhombic minerals with chemical compositions which represent a quasi-binary solution close to the join between FeSiO₃ and MgSiO₃. The ferrous and magnesium ions occur at two nonequivalent, octahedrally coordinated sites *M1* and *M2*, with Fe²⁺ preferring *M2*. The cation exchange is formulated by the simple relation



The energy difference between the two opposing reactions determines the temperature range in which ordering and disordering will occur under equilib-

rium conditions. If the activation energy needed to overcome the barriers for cationic diffusion within the crystal structure is high, the time necessary to reach equilibrium will be long. No change of lattice symmetry occurs in this simple order-disorder transition.

We have determined precise site occupancy numbers for Fe²⁺ at *M1* and *M2* from the quadrupole split doublets of ⁵⁷Fe observed in gamma-ray resonant absorption spectra at 77°K (1). Orthopyroxenes with various compositions were heat-treated at different temperatures. The data were analyzed as follows. The fraction of Fe²⁺ at *M1* and *M2* is proportionally related to the ratio of the areas under the two doublets provided that thin absorbers are used and the recoilless fraction of ⁵⁷Fe is the same at both sites. Four Lorentzian curves were fitted to the data by the least-squares method (13 variable fits). A careful analysis of many spectra showed that the intrinsic widths of all four peaks are very nearly the same. Therefore, since peak heights are determined much more precisely than line widths, ratios of the peak heights were used rather than ratios of the product of peak height times width. Data for one orthopyroxene are given in Table 1 (which shows three spectra of the same absorber).

Figure 1 shows the equilibrium Fe²⁺,Mg distribution over sites *M1* and *M2* at 1000°C. In the range 0 ≤ *x* < 0.6, where *x* is the ratio Fe²⁺/(Fe²⁺ + Mg) of the crystal, the observed site occupancy is in excellent agreement with ideal distribution assumed for each site (2, 3). The site occupancy numbers *X*₁ and *X*₂ for Fe²⁺ at *M1* and *M2*, respectively, are in accordance with the hyperbolic relation

$$k = X_1(1 - X_2)/X_2(1 - X_1) \quad (2)$$

where *k* is the equilibrium constant. In the region 0.7 < *x* ≤ 1.0 (Fig. 1), there is a typical deviation from ideal distribution. At 1000°C, orthopyroxenes are still far from completely disordered. No additional disorder could be observed, however, when crystals were heated at higher temperatures. Equilibrium values of order-disorder were also determined for a sample with *x* = 0.574 at 800°, 700°, 600°, and 500°C. The variation of the site occupancy number *X*₂ with temperature is shown in Fig. 2.

Data for orthopyroxenes from slowly annealed metamorphic and plutonic rocks are plotted in Fig. 1. These samples exhibit site occupancy numbers close to an equilibrium distribution

Table 1. Ferrous iron site occupancy determined from ^{57}Fe Mössbauer spectra. The spectra of orthopyroxenes exhibit two distinct nuclear quadrupole split doublets due to Fe^{2+} at the octahedrally coordinated sites $M1$ and $M2$. The low-velocity peaks of each doublet are designated A and the high-velocity peaks B . The doublet of ^{57}Fe at $M1$ (A_1B_1) shows the larger splitting. The fraction of Fe^{2+} at $M1$ (referred to total Fe^{2+} at $M1$ and $M2$) is equal to the peak height ratio $[I(A_1) + I(A_2)]/[I(A_1) + I(A_2) + I(B_1) + I(B_2)]$ provided that the intrinsic line width of all four peaks is the same. Site occupancy numbers of Fe^{2+} are obtained by multiplication of the Fe^{2+} fractions at $M1$ and $M2$ by $2[\text{Fe}^{2+}/(\text{Fe}^{2+} + \text{Mg})]$. The table shows the results of three spectra of one absorber.

Spectrum of sample	Line widths (full width at half height) (mm/sec)				Intensities referred to $I(A_1 + A_2 + B_1 + B_2)$				Fraction of Fe^{2+} in $M1$	Fe $^{2+}$ site occupancy numbers	
	B_1	B_2	A_2	A_1	$I(B_1)$	$I(B_2)$	$I(A_2)$	$I(A_1)$		$X_1(M1)$	$X_2(M2)$
V2	0.254	0.281	0.275	0.255	0.186	0.298	0.342	0.173	0.360	0.502	0.894
V9	.295	.314	.313	.286	.185	.302	.343	.170	.355	.495	.901
V41	.260	.289	.280	.273	.187	.302	.343	.168	.356	.495	.901
Average	.270	.295	.289	.271					.356	.498	.899
S.E.	$\pm .018$	$\pm .014$	$\pm .017$	$\pm .013$					$\pm .002$	$\pm .003$	$\pm .003$

curve which corresponds to about 480°C (compare the plot of the unheated sample 3209 in Fig. 2). We believe that there is an "energy barrier" close to 480°C which prevents further ordering. Orthopyroxenes from rapidly cooled volcanic rocks occur between the limits for maximum disorder and maximum order; their site occupancy numbers scatter around the equilibrium isotherm at 600°C .

Heat treatments at constant temperature over various periods of time make possible the determination of the rates for the disordering or ordering reaction and activation energies for the diffusion processes. For the region

$0 \leq x < 0.6$ of the solid solution, where thermodynamics derived from an ideal distribution seems to be appropriate, it is reasonable to assume a rate equation of the form

$$-\frac{dX_2}{dt} = -K_{12}X_1(1 - X_2) + K_{21}X_2(1 - X_1) \quad (3)$$

where K_{21} and K_{12} are the rate constants for isothermal disordering and ordering, respectively. According to Eqs. 2 and 3

$$K_{21}/K_{12} = k$$

Experiments at 500° and 1000°C yielded estimates of the rate constants for disordering at these temperatures. From these values, the average activation energies for disordering (E_{aD}) and for ordering (E_{aO}) can be calculated from the Arrhenius relation if we assume that these energies are approximately invariant between 500° and 1000°C . The magnitudes are $E_{aD} \approx 20$ kcal per mole and $E_{aO} \approx 15$ kcal per

mole [formula unit $(\text{Fe},\text{Mg})_2\text{Si}_2\text{O}_6$]. The equilibrium constants k at 800° , 700° , 600° , and 500°C were approximately determined. From the relation

$$\Delta G_E^0 = -RT \ln k$$

(where R is the gas constant and T is the absolute temperature) it is found that the standard Gibbs free-energy difference ΔG_E^0 for reaction 1 is nearly constant from 500° to 1000°C , the average value being 3.6 kcal per mole. This is in fair agreement with

$$\Delta G_E^0 \approx E_{aD} - E_{aO}$$

thus showing that the assumptions implied in the Arrhenius relation are within reason.

The low activation energies for Fe^{2+} , Mg diffusion in orthopyroxenes are surprising. It would be of interest to know whether this generally applies to cationic exchange among octahedrally coordinated sites in chain silicates. The activation energies, for instance, for Al,Si diffusion among the tetrahedral sites in alkali feldspars, are considerably higher. Thus, the rates of ordering in orthopyroxenes can be expected to be relatively rapid. In fact, unlike Al,Si ordering in silicates, Fe^{2+} ,Mg ordering in orthopyroxenes can be achieved experimentally at rather low temperatures within reasonable periods of time. A sample with $\text{Fe}^{2+}/(\text{Fe}^{2+} + \text{Mg}) = 0.574$, previously disordered at 900°C with $X_2 = 0.73$, was found to be more ordered with $X_2 = 0.78$ after heat treatment for 7 days at 500°C . By use of an empirical rate equation similar to Eq. 1 determined by additional ordering experiments, one can calculate the temperature and time dependence of site occupancy.

Our kinetics experiments demonstrate that equilibrated cation distributions will be readily attained at the tem-

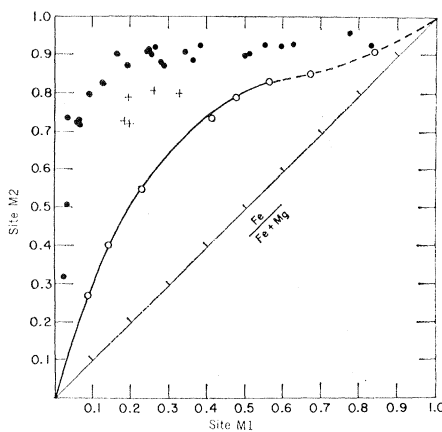


Fig. 1 (above left). Plot of Fe^{2+} site occupancy at $M1$ against $M2$ of orthopyroxenes. ●, Samples from metamorphic and plutonic rocks; +, samples from volcanic rocks; ○, natural samples heated at 1000°C until equilibrium Fe^{2+} ,Mg distribution was achieved and quenched. The solid line is a least-squares fit to Eq. 2; equilibrium constant $k(1000^\circ\text{C}) = 0.235$.

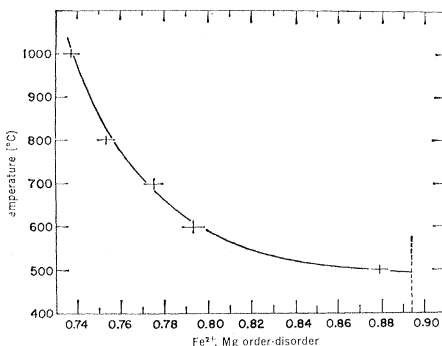


Fig. 2 (bottom left). Plot of Fe^{2+} ,Mg order-disorder as a function of temperature for sample 3209 [$\text{Fe}^{2+}/(\text{Fe}^{2+} + \text{Mg}) = 0.574$]. The points refer to equilibrium values determined from kinetic experiments at each temperature. By use of these equilibrium values and Eq. 2, hyperbolic curves for 800° , 700° , 600° , and 500°C can be drawn in Fig. 1 for values of $\text{Fe}^{2+}/(\text{Fe}^{2+} + \text{Mg})$ between 0 and ~ 0.50 . The vertical dashed line refers to the site occupancy number X_2 for the unheated sample 3209.

peratures of crystallization. Because of the predicted rapid rates of ordering at high temperature, deviations from equilibrated distributions are not expected at those temperatures. However, in rapidly cooled volcanic rocks it seems likely that the rearrangement of cations at temperatures somewhat above the limiting temperature of $\approx 480^\circ\text{C}$ for maximum order may not follow equilibrium conditions and that metastable cation distributions will be quenched. In view of the varying rates of cooling of volcanic rocks, it seems probable that the range of metastable distributions may actually be wider than that shown in Fig. 1. The effect of diluted foreign cations like Mn, Ca, Al, and so forth, on site occupancy numbers for Fe^{2+} at M1 and M2 and the rate constants are still unknown.

Our experimentally determined equilibrium temperatures for intracrystalline ordering at approximately 480°C in some metamorphic and igneous rocks can be compared with other data obtained from intercrystalline distributions and exsolution phenomena. The Fe^{2+} , Mg distribution between coexisting orthopyroxene and clinopyroxene phases generally reflect crystallization temperatures for metamorphic and intrusive igneous rocks (4). McCallum (5) determined distribution coefficients for intercrystalline exchange in pyroxenes from the Stillwater complex, Montana. He found distribution coefficients between those of unexsolved orthopyroxene and clinopyroxene corresponding to magmatic temperatures (1100° to 1200°C), but values for exsolved coarse-size lamellae and the host crystals gave temperatures in the range 600° to 800°C . Apparently there is an adjustment of the Fe^{2+} , Mg distribution between the exsolved phase and the host toward equilibrium at successively lower temperatures. It is reasonable to assume that, while cation migration occurs on the scale of microns in the case of exsolution phenomena, intercrystalline exchange involving distances of millimeters or centimeters is not possible during cooling of the rock. However, ordering of cations observed from Mössbauer studies of site occupancy involves distances of a few lattice constants and presumably takes place at much lower temperatures.

STEFAN S. HAFNER
DAVID VIRGO

Department of Geophysical Sciences,
University of Chicago,
Chicago, Illinois 60637

References and Notes

1. D. Virgo and S. S. Hafner, *Earth Planet. Sci. Lett.* **4**, 265 (1968).
2. R. F. Mueller, *Geochim. Cosmochim. Acta* **26**, 581 (1962).
3. S. Ghose and S. S. Hafner, *Z. Kristallogr.* **125**, 157 (1967).

4. R. Kretz, *J. Geol.* **71**, 773 (1963).
5. I. S. McCallum, thesis, University of Chicago (1968).
6. Supported by the NSF (Ga-1134), NASA (NAS-9-8080), and NASA (NSG-366 awarded to Dr. E. Anders).

7 March 1969

Elastic Coefficients of Animal Bone

Abstract. *The elastic stiffness coefficients of dried bovine phalanx and femur and of fresh bovine phalanx were measured by an ultrasonic technique. An analysis of the crystallographic structure of the principal components of bone and its piezoelectric and pyroelectric behavior showed that bone is a texture that has the same elastic coefficient matrix as a hexagonal single crystal. The five elastic stiffness coefficients of fresh phalanx are: C_{11} , 1.97; C_{12} , 1.21; C_{13} , 1.26; C_{33} , 3.20; and C_{44} , 0.54 (all in units of 10^{11} dynes per square centimeter). Value of axial and transverse Young's and shear moduli, compressibility, and the three Poisson's ratios were calculated.*

It has been proposed that the electro-mechanical effect (electrical potential generated by application of mechanical stress) observed in bone may have important physiological functions (1, 2). Some processes in which this effect may be significant include bone remodeling, diffusional processes in bone nourishment, and hearing. To study these processes, one must understand the effect of mechanical stress on bone, that is, understand the elastic behavior of bone. In an attempt to find measurements of the elastic constants of bone in the literature, I discovered that all of the elastic data on bone had been measured by static techniques; that is, the bone was sufficiently stressed by tension, compression, or torsion so that measurably large displacements could be observed. This technique has two serious defects. First, the stress-strain relationship of bone is nonlinear (3). In order for the strain to be large enough to be measurable in a static test, it may be necessary to stress the bone into the nonlinear stress-strain region, thus yielding a meaningless result. Second, bone is a highly anisotropic material (4). It is not possible to characterize fully the elastic properties of such a material with only two or three technical elastic moduli, such as the axial Young's modulus or the axial shear modulus.

It was desired to determine elastic constants free of these two defects. Therefore, the structure of bone was analyzed in terms of a polycrystalline texture to determine the number and type of independent elastic constants. An ultrasonic technique was developed for the measurement of the constants, and statistical methods were used for

the analysis of the results. From these results, the Young's modulus and the shear modulus as functions of direction relative to the bone axis were calculated. In this report I describe the method and the results of measurements on specimens of dried and fresh bovine bones.

The elastic properties of a material can be completely described by the components of the elastic stiffness matrix (C_{ij}). The elastic stiffnesses are the linear coefficients of proportionality between the stress matrix (σ_i) and the strain matrix (ϵ_j):

$$(\sigma_i) = (C_{ij})(\epsilon_j) \quad (i, j = 1, 2, \dots, 6) \quad (1)$$

When the i and j are equal to 1, 2, or 3, the symbols σ_i and ϵ_j refer to normal stresses and strains, respectively, in the crystallographic 1, 2, or 3 directions. The subscripts 4, 5, and 6 refer to shear stresses or strains (5). A consideration of the crystal structure of the major components of bone, hydroxyapatite (6) and collagen (7), and the piezoelectric (8) and pyroelectric (9) characteristics of bone suggested that it should behave elastically as a hexagonal material. In such a material (5), the elastic stiffness matrix takes the following form:

$$\begin{array}{cccccc} C_{11} & C_{12} & C_{13} & 0 & 0 & 0 \\ C_{12} & C_{11} & C_{13} & 0 & 0 & 0 \\ C_{13} & C_{13} & C_{33} & 0 & 0 & 0 \\ 0 & 0 & 0 & C_{44} & 0 & 0 \\ 0 & 0 & 0 & 0 & C_{44} & 0 \\ 0 & 0 & 0 & 0 & 0 & \frac{1}{2}(C_{11}-C_{12}) \end{array}$$

Thus the elastic behavior of bone is characterized by five independent coefficients.

The coefficients were calculated (10) from measurements of the velocities of shear and longitudinal ultrasonic waves